Thermal conductivity measurements and correlations of pure R1243zf and binary mixtures of R32 + R1243zf and R32 + R1234yf

Dongchan Kim[1, 5], Hangtao Liu[2], Xiaoxian Yang[1], Fufang Yang[3, 6], Jackson Morfitt[1], Arash Arami-Niya[1, 4], Mincheol Ryu[5], Yuanyuan Duan[2], Eric F. May[1,*]

[1] Fluid Science & Resources Division, Department of Chemical Engineering, University of Western Australia, Crawley, WA 6009, Australia

[2] Key Laboratory for Thermal Science and Power Engineering of Ministry of Education, Beijing Key Laboratory for CO2 Utilization and Reduction Technology, Tsinghua University, Beijing 100084, China

[3] Center for Energy Resources Engineering (CERE), Department of Chemical and Biochemical Engineering, Technical University of Denmark, 2800 Kgs. Lyngby, Denmark

[4] Discipline of Chemical Engineering, Western Australian School of Mines: Minerals, Energy and Chemical Engineering, Curtin University, GPO Box U1987, Perth, WA 6845, Australia

[5] Naval & Energy System R&D Institute, Energy System R&D Department, Daewoo Shipbuilding and Marine Engineering Co. Ltd., 3370, Geoje-daero, Geoje-si, Gyeongsangnam-do, Korea

[6] IFP Energy Nouvelles, 1 et 4 Avenue de Bois-Préau, 92852 Rueil-Malmaison Cedex, France

Abstract

Thermal conductivity measurements of pure R1243zf and binary mixtures of R32 + R1243zf and R32 + R1234yf were conducted in the homogeneous liquid and vapour phases with a transient hot-wire technique. The mole fractions of R32 are 0.25, 0.50, and 0.75 in both binary systems. The temperature range of the measurements was from (264.1 to 405.6) K with pressures ranging between (0.9 and 6.1) MPa. The transient hot-wire apparatus was validated with measurements of pure CO_2 in both the liquid and vapour regions. The relative combined expanded uncertainty (k = 2) in the experimental thermal conductivity was approximately 2.0%. The relative deviations of the measured thermal conductivities from those calculated using the extended corresponding states (ECS) model as implemented in the software REFPROP 10 were between (−13 and 10)% in the vapour phase, and between (−14 and 1)% in the liquid phase. Additionally, the performance of a new approach to predicting fluid transport properties, the residual entropy scaling model incorporating the cubic-plus-association equation of state (RES-CPA model) was tested for these mixtures by first determining the scaling parameter of pure R1243zf. The RES-CPA model was then able to predict the mixture thermal conductivities generally within 10%, which is similar to the ECS model; however no additional parameters were introduced to the RES-CPA model to describe binary interactions.

Keywords: Thermal conductivity, transient hot-wire, R32, R1234yf, R1243zf

[*]Corresponding author. *Email address:* eric.may@uwa.edu.au.

Highlights

- Thermal conductivities of R32+R1234yf and R32+R1243zf mixtures were measured.
- Measurements were conducted from (264.1 to 405.6)K up to 6.1MPa.
- Relative combined expanded uncertainties (k = 2) in thermal conductivity are 2.0%.
- Parameters of the RES-CPA model for pure R1243zf and R32 + R1243zf were fitted.
- Relative deviations from the ECS and RES-CPA models are generally within 10%.

Thermal conductivity measurements and correlations of pure R1243zf and binary mixtures of R32 + R1243zf and R32 + R1234yf

Dongchan Kim[1, 5], Hangtao Liu[2], Xiaoxian Yang[1], Fufang Yang[3, 6], Jackson Morfitt[1], Arash Arami-Niya[1, 4], Mincheol Ryu[5], Yuanyuan Duan[2], Eric F. May[1,*]

[1] Fluid Science & Resources Division, Department of Chemical Engineering, University of Western Australia, Crawley, WA 6009, Australia

[2] Key Laboratory for Thermal Science and Power Engineering of Ministry of Education, Beijing Key Laboratory for CO2 Utilization and Reduction Technology, Tsinghua University, Beijing 100084, China

[3] Center for Energy Resources Engineering (CERE), Department of Chemical and Biochemical Engineering, Technical University of Denmark, 2800 Kgs. Lyngby, Denmark

[4] Discipline of Chemical Engineering, Western Australian School of Mines: Minerals, Energy and Chemical Engineering, Curtin University, GPO Box U1987, Perth, WA 6845, Australia

[5] Naval & Energy System R&D Institute, Energy System R&D Department, Daewoo Shipbuilding and Marine Engineering Co. Ltd., 3370, Geoje-daero, Geoje-si, Gyeongsangnam-do, Korea

[6] IFP Energy Nouvelles, 1 et 4 Avenue de Bois-Préau, 92852 Rueil-Malmaison Cedex, France

To be submitted to *International Journal of Refrigeration* (2021)

Abstract

Thermal conductivity measurements of pure R1243zf and binary mixtures of R32 + R1243zf and R32 + R1234yf were conducted in the homogeneous liquid and vapour phases with a transient hot-wire technique. The mole fractions of R32 are 0.25, 0.50, and 0.75 in both binary systems. The temperature range of the measurements was from (264.1 to 405.6) K with pressures ranging between (0.9 and 6.1) MPa. The transient hot-wire apparatus was validated with measurements of pure CO_2 in both the liquid and vapour regions. The relative combined expanded uncertainty (k = 2) in the experimental thermal conductivity was approximately 2.0%. The relative deviations of the measured thermal conductivities from those calculated using the extended corresponding states (ECS) model as implemented in the software REFPROP 10 were between (−13 and 10)% in the vapour phase, and between (−14 and 1)% in the liquid phase. Additionally, the performance of a new approach to predicting fluid transport properties, the residual entropy scaling model incorporating the cubic-plus-association equation of state (RES-CPA model) was tested for these mixtures by first determining the scaling parameter of pure R1243zf. The RES-CPA model was then able to predict the mixture thermal conductivities generally within 10%, which is similar to the ECS model; however no additional parameters were introduced to the RES-CPA model to describe binary interactions.

Keywords: Thermal conductivity, transient hot-wire, R32, R1234yf, R1243zf

*Corresponding author. *Email address:* eric.may@uwa.edu.au.

Nomenclature list

Abbreviations

CPA	Cubic-plus-association
ECS	Extended corresponding states
EoS	Equation of state
G	Gas
GWP	Global warming potential
HFC	Hydrofluorocarbon
HFO	Hydrofluoroolefin
L	Liquid
ODP	Ozone depletion potential
R1234yf	2,3,3,3-Tetrafluoropropene
R1243zf	3,3,3-Trifluoroprop-1-ene
R32	Difluoromethane
RES	Residual entropy scaling
SC	Supercritical region

Symbols

B_1, B_2, B_3, B_5, B_0, and B_{-1}	coefficients in the univariate function of λ^* with s^{res}
k	coverage factor
k_{ij}	binary interaction parameter
M	molar mass
p	pressure, Pa
q	heat flux per unit length, $W \cdot m^{-1}$
R	universal gas constant, $J \cdot mol^{-1} \cdot K^{-1}$
r_o	radius of the wire, m
s^{res}	residual entropy, $J \cdot mol^{-1} \cdot K^{-1}$
t	time, s
T	temperature, K
ΔT	temperature rise of the wire, K
u	standard uncertainty
U	expanded uncertainty
U_C	combined expanded uncertainty
V	induced voltage, V
x	mole fraction

Greek symbols

ζ	fluid-specific entropy scaling parameter
η^o	dilute gas viscosity, Pa·s
λ	thermal conductivity,$W \cdot m^{-1} \cdot K^{-1}$
λ^*	reduced thermal conductivity
λ^o	dilute gas thermal conductivity,$W \cdot m^{-1} \cdot K^{-1}$
ρ	density, $kg \cdot m^{-3}$
ρ_{EoS}	density calculated with EoS, $kg \cdot m^{-3}$
κ	thermal diffusivity
γ	Euler constant

1. Introduction

Many countries are taking actions to adopt more eco-friendly refrigerants with low ozone depletion potential (ODP) and low global warming potential (GWP) (Abas et al., 2018; Calm, 2008). Fourth generation refrigerants, including hydrofluorocarbons (HFCs) and hydrofluoroolefins (HFOs), are attracting increasing attention due to their low GWP and are being used increasingly in air-conditioning systems for houses and automobiles (Kim et al., 2020). In particular, the HFOs R1234yf (2,3,3,3-Tetrafluoropropene) and R1243zf (3,3,3-Trifluoroprop-1-ene) have negligibly-small GWP (see Table 1) (McLinden et al., 2000; Zilio et al., 2011) compared to the commonly-used refrigerant R134a (1,1,1,2-Tetrafluoroethane) that has a GWP of 1300 (Higashi et al., 2018; Pal et al., 2018). Both HFOs are considered potential alternatives to R134a as they have similar phase envelopes, and similar coefficients of performance for the heating, ventilation and air conditioning (HVAC) systems (Gil and Kasperski, 2018; Kujak and Schultz, 2016; Lai, 2014). However, pure refrigerants inevitably have one or more disadvantages and, furthermore, HFOs are generally mixed with other refrigerants to reduce their slight flammability while retaining the environmental advantages (Wu et al., 2019).

Table 1. Information for the pure fluid samples used in this work.

ASHRAE name	IUPAC name	CAS #	Source	Purity/mole fraction	ODP[c]	GWP_{100}[c]
R32	Difluoromethane	75-10-5	Coregas	0.995[a]	0	677
R1234yf	2,3,3,3-Tetrafluoropropene	754-12-1	Coregas	0.995[a]	0	< 1
R1243zf	3,3,3-Trifluoroprop-1-ene	677-21-4	Coregas	0.995[a]	0	< 1
R744 (CO_2)	Carbon Dioxide	124-38-9	Coregas	0.99995[b]	0	1

[a] Impurity information was provided by the supplier and no further purification was done.
[b] Impurities (stated by supplier): $x(H_2O) \leq 7\times10^{-6}$, $x(O_2) \leq 1\times10^{-5}$, x(other C_mH_n) $\leq 5\times10^{-6}$, $x(CO) \leq 2\times10^{-6}$, where x denotes mole fraction. No further purification was done.
[c] ODP: Ozone depletion potential, GWP_{100}: 100-year Global warming potential (Pachauri et al., 2014)

The thermal conductivity of refrigerants is crucial to the design of heat transfer equipment, such as boilers and heat exchangers. When accurate values of thermal conductivity of the refrigerant are not available, such equipment is normally over-sized to ensure that the amount of heat targeted by the design can in fact be transferred (Kujak and Schultz, 2016; Webb, 1981). Accordingly, accurate values of refrigerant thermal conductivity can help optimize the size of equipment and thus reduce the capital cost of construction. In this work, we focus on the thermal conductivity of pure R1243zf and binary systems of R1243zf or R1234yf with R32 (Difluoromethane). R32 is also flammable; however, mixtures of R32 and HFOs are can often

help make the refrigerant less flammable (Sadaghiani et al., 2021). The present measurements, in which the mole fractions of R32 in the binary mixtures were 0.25, 0.50 and 0.75 builds upon our previous work (Kim et al., 2020) where eight equimolar binaries and two multi-component mixtures containing HFOs, HFCs and CO_2 (natural refrigerant) were investigated.

No thermal conductivity data for pure R1243zf and binary mixtures of R32 + R1243zf are available in the literature. Only one data source (Miyara et al., 2011) of the binary R32 + R1234yf system at a R32 mole fraction of 0.661 in the temperature range from (283 to 298) K and pressure range from (0.1 to 1.2) MPa is available. Here thermal conductivity measurements were carried out in the homogeneous liquid and vapour phases with a transient hot-wire technique in the temperature range from (264.1 to 405.6) K with pressures ranging between (0.9 and 6.1) MPa. The experimental data were compared to the extended corresponding states (ECS) model (Chichester and Huber, 2008) implemented in REFPROP 10 software package (Lemmon et al., 2018), as well as the residual entropy scaling model incorporating a cubic-plus-association (RES-CPA) equation of state (EoS). The RES-CPA model was recently adapted for the viscosity (Liu et al., 2020; Yang et al., 2021) and thermal conductivity (Liu et al., 2021) of HFCs, HFOs, and their binary mixtures. In this work, the RES-CPA approach is extended to describe the thermal conductivity of pure R1243zf and the mixtures measured here.

2. Experimental

2.1. Measurements

A transient-hot wire apparatus based on the design developed by Perkins et al. (1991) (Perkins et al., 1991) was used in this work, as shown in Figure 1. The experimental setup, measurement principle and measurement procedure were explained in detail previously (Kim et al., 2020; Mylona et al., 2019; Mylona et al., 2020). Here we only present key information regarding the measurement principle and measurement procedure.

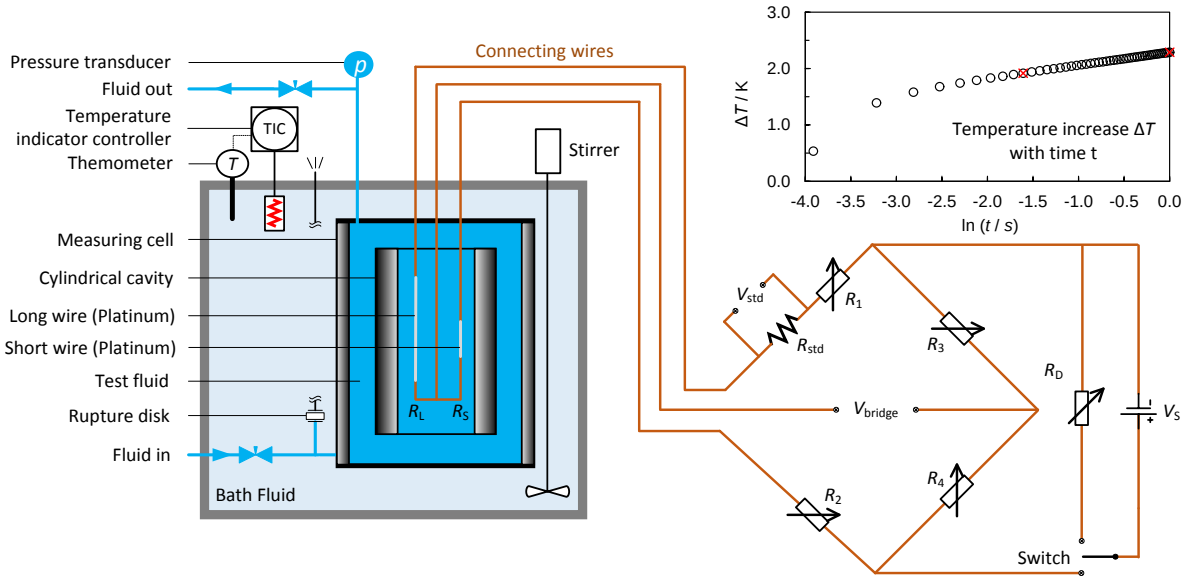

Figure 1. Schematic diagram of the measuring system

The transient hot-wire method is an absolute method (Assael et al., 2010; Perkins et al., 2016) from which the thermal conductivity is calculated based on the transient temperature increase of a wire when a step voltage is applied. A constant heat flux per unit length, q, is generated along the wire, which produces a temperature rise, ΔT, as a function of time t. Assael et al. (1991) presented an ideal model for ΔT based on an infinitely-long vertical wire of zero heat capacity and infinite thermal conductivity immersed in the fluid. According to the ideal model, ΔT changes linearly as a function of the logarithm of time, with a slope that depends on the fluid's thermal conductivity. Specifically, the transient temperature increase of the ideal wire is given by

$$\Delta T\left(r_0,t\right)=\frac{q}{4\pi\lambda}\ln\left(\frac{4\kappa t}{r_0^2 e^{\gamma}}\right) \tag{1}$$

where λ is the fluid's thermal conductivity, r_o is the radius of the wire, κ is the fluid's thermal diffusivity, and $\gamma = 0.57721566\ldots$ is the Euler constant.

Equation (1) is derived from an idealised model; suitable experimental design and measurement conditions are necessary to minimize the departures of any real measurement from the ideal model. Even with such careful design, three main corrections are needed to reconcile the ΔT measured with that predicted using Eq. (1). These include: the finite heat capacity of the wire, the finite boundaries associated with the dimensions of the wire and cylindrical pressure vessel, and the effect of radiation. Details of these corrections for the apparatus used in this work have been presented previously (Kim et al., 2020; Mylona et al.,

2020) and the impact of these corrections to the thermal conductivity measured here are discussed in section 4.1.

In mixture measurements, it is extremely important to ensure that no phase transition occurs under any circumstances. Kim et al. (2020) provided a detailed description about the measurement procedures used to ensure the fluid remained as either a single liquid or vapor phase. At each temperature and pressure condition, at least six experiments were repeated with the power supply voltage in the range of (2 – 6) V, producing an experimental temperature rise of (1 – 2) K to minimize the impacts of natural convection and electrical noise (Kim et al., 2020).

2.2. Experimental materials

The pure fluid samples were provided by Coregas, with purities in mole fraction of 0.995 for R32, R1234yf and R1243zf. They were used as received from the supplier without further gas analysis or purification. Detailed information for the sample refrigerants is listed in Table 1. The binary mixtures were prepared volumetrically in our laboratory following the preparation procedure described by Al Ghafri et al. (2019). The mole fraction compositions of the mixtures prepared here are listed in Table 2, together with the expanded uncertainty (k = 2). The uncertainties are in the range of 0.018 to 0.020 mole fraction as determined by the method described previously (Arami-Niya et al., 2020; Yang et al., 2020a). Note that unless otherwise stated, all uncertainties in this work are expanded uncertainties (k = 2) with a confidence level of 95%.

Table 2. Mole fraction compositions of the mixtures prepared. The numbers in parentheses indicate the expanded (k = 2) uncertainty in the last two digits of the reported mole fraction.

Mixtures	Components/mole fraction		
	R32	R1234yf	R1243zf
1	$0.500_{(18)}$	$0.500_{(18)}$	-
2	$0.252_{(18)}$	$0.748_{(18)}$	-
3	$0.750_{(18)}$	$0.250_{(18)}$	-
4	$0.500_{(18)}$	-	$0.500_{(18)}$
5	$0.248_{(20)}$	-	$0.752_{(20)}$
6	$0.750_{(18)}$	-	$0.250_{(18)}$

2.3. Uncertainty analysis

According the “Guide to the Expression of Uncertainty in Measurement” (ISO and OIML, 1995), the uncertainty of the measured thermal conductivity was estimated by considering the measured quantities, parameters, calculations and compositions of the fluids. A detailed

uncertainty analysis was given previously (Kim et al., 2020; Mylona et al., 2020). A budget for the combined, expanded uncertainty of the thermal conductivities $U_C(\lambda)$ measured here is listed in

Table **3** with the measurement of the mixture (0.252 R32 + 0.748 R1234yf) at T = 287.17 K and p = 2.43 MPa taken as an example condition. The uncertainty in the composition of the prepared mixtures, the simplification and corrections applied to the data to enable use of the ideal model, and the scatter of repeated measurements are the dominant factors contributing to the overall uncertainty. Across all conditions measured, the combined relative uncertainty $U_C(\lambda)/\lambda$ was approximately 2.0% for all mixtures.

Table 3. Uncertainty budget for the thermal conductivity. The contributions refer to the measurement of (0.252 R32 + 0.748 R1234yf) at T = 284.17 K and p = 2.43 MPa.[a]

Source	Uncertainty U	Contribution to $U_C(\lambda)/\lambda$
Temperature	100 mK	0.01%
Voltage on standard resistor	0.02%	0.02%
Bridge imbalance	0.3%	0.30%
Variable resistor	0.05%	0.03%
Power supply	0.1%	0.20%
Wire radius (5.0 μm)	0.1 μm	0.02%
Heat capacity of the wire	2.0%	0.03%
The standard resistor	0.1%	0.10%
Resistance of the long wire	0.1%	0.05%
Resistance of the short wire	0.2%	0.14%
Resistance of the working wire	0.3%	0.30%
Length of the long wire (0.1515 m)	0.0002 m	0.19%
Length of the short wire (0.0466 m)	0.0002 m	0.18%
Regression	10% of data	0.20%
Composition	0.018 mole frac.	1.08%
Simplification & correction of the ideal model Eq. (1) [b]	1.0%	1.00%
Scatter of the repeated measurements	1.1%	1.18%
Summary: Combined uncertainty for this mixture $U_C(\lambda)/\lambda$		1.98%

[a] Uncertainty contributions to $U_C(\lambda)$ associated with pressure measurement p, and other parameters (Mylona et al., 2020) are less than 0.01%.

[b] The major simplifications and corrections to the ideal model are those associated with the two-wire technique, the finite heat capacity of the wire, and the boundary confining the fluid to a finite space, including the effect of radiation. See Mylona et al. (2020) and Kim et al. (2020) for futher detail.

3. Modelling

In the residual entropy scaling (RES) approach, transport property data that depend on temperature, density, and composition, are mapped into a univariate function of the residual

entropy. Several authors have shown that experimental transport data can be readily correlated with the RES approach (Bell, 2020; Fouad, 2020; Hopp and Gross, 2019; Yang et al., 2020b). The residual entropy scaling law incorporating the cubic-plus-association EoS (RES-CPA model) was developed to correlate the thermal conductivity of HFCs, HFOs, and their binary mixtures previously (Liu et al., 2021). The model defined the reduced thermal conductivity λ^* as

$$\lambda^* = \frac{\lambda}{\lambda^{o} \cdot \exp\left(-\frac{s^{res}}{R}\right) + \eta^{o} \cdot \frac{15R}{4M} \cdot \left(1 - \exp\left(-\frac{s^{res}}{R}\right)\right)} \tag{2}$$

and λ^* was expressed as a univariate function of residual entropy s^{res} as

$$\ln \lambda^* = B_1 \cdot \left(\frac{s^{res}}{\zeta R}\right)^{\frac{1}{3}} + B_2 \cdot \left(\frac{s^{res}}{\zeta R}\right)^{\frac{2}{3}} + B_3 \cdot \left(\frac{s^{res}}{\zeta R}\right) + B_5 \cdot \left(\frac{s^{res}}{\zeta R}\right)^{\frac{5}{3}} + B_{-1} \cdot \left[\exp\left(-B_0 \cdot \frac{s^{res}}{\zeta R}\right) - 1\right] \tag{3}$$

In Eqs. (2) and (3), λ^o is the dilute gas thermal conductivity, η^o is the dilute gas viscosity, R = 8.3144626 J·K^{-1}·mol^{-1} is the universal gas constant, M is the molar mass, ζ is a fluid-specific rescaling parameter, and B_1, B_2, B_3, B_5, B_0, and B_{-1} are universal coefficients for all the HFCs and HFOs investigated (Liu et al., 2021). The dilute gas transport properties, λ^o and η^o, were obtained using kinetic theory (Neufeld et al., 1972). The residual entropy is a function of thermodynamic state and was derived from the CPA EoS. The rescaling parameter ζ was determined for each pure fluid by regressing the available data for each to a single, universal RES curve. The coefficients B_i and the rescaling parameter ζ for pure R32 and pure R1234yf were determined by Liu et al (2021), while ζ for pure R1243zf was obtained here from the data measured in this work. For the binary mixtures, the rescaling parameter ζ was estimated via a mole fraction weighted average of the pure component parameters. The only mixture-specific parameter is the binary interaction parameter contained within the van der Waals mixing rule used by the CPA EoS. This is often obtained by fitting to vapour-liquid-equilibrium and/or other thermodynamic property data for that mixture and was not adjusted here. This is in contrast to the ECS model, which contains up to three binary-specific interaction parameters for the description of mixture transport properties (Chichester and Huber, 2008); these are in addition to any binary interaction parameters used in the equation of state used to determine the mixture density as an input to the ECS model.

4. Results and Discussion

4.1. Validation tests

The validation tests of the experimental apparatus were carried out with pure CO_2 at pressures from (0.4 to 8.1) MPa and temperatures between (234.3 and 397.9) K previously (Kim et al., 2020). In this work, based on one of those validation tests of CO_2 near its critical temperature, we present additional information regarding the extent to which each correction factor (see section 2.1) affects the results. The experimental temperature increase of the wire ΔT as a function of time t and logarithm time $\ln(t)$ is displayed in Figure 2 (a) and (b), respectively, together with the three corrections. The finite heat capacity of the wire and the effect of radiation contributed corrections up to 0.06 K, which was appreciable compared to that of the finite boundaries (negligibly small), yet still small compared to the total temperature increase of 2.2 K. In particular, the effect of radiation becomes significant in the vicinity of the critical point. According to Figure 2 (c), which illustrates the relative deviations of ΔT values from the fit to Eq. (1) as a function of time $\ln(t)$, the correction of the radiation effect clearly improved the linearity of the relationship between ΔT and $\ln(t)$.

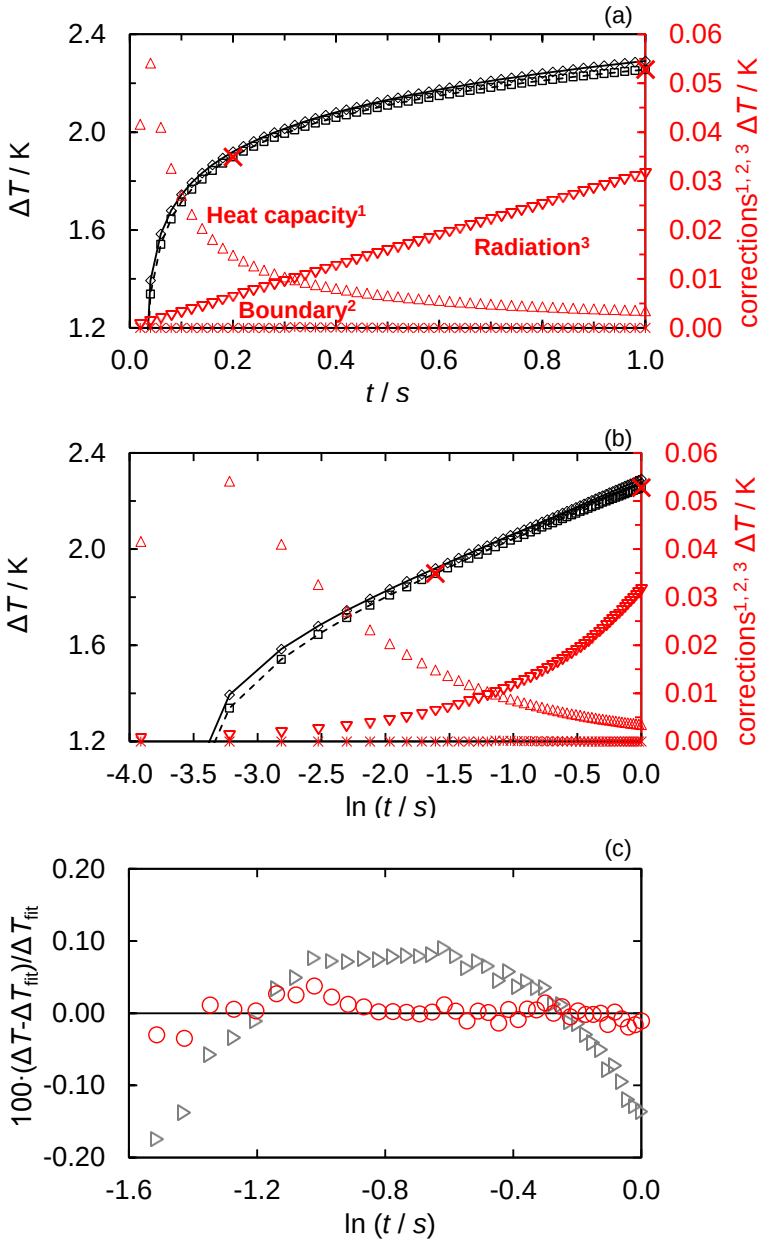

Figure 2. (a) and (b), The temperature increase of the wire ΔT as a function of time t and ln(t), respectively, for a pure carbon dioxide measurement at T = 313.15 K and p = 4.05 MPa. Symbol: (left axis) □ no corrections applied, ◇ all three corrections applied, × data points corresponding to the start and end times used for the fit; (right axis) corrections with △ the finite heat capacity of the wire, ✳ the finite outer boundary, and ▽ the radiation effect. (c) Relative deviations of the temperature increase of the wire ΔT values from the fit ΔT_{fit} to Eq. (1). ▷, only corrections associated with the finite heat capacity of the wire and outer boundary corrections were applied; ○, the radiation correction applied additionally.

4.2. Measurement results for pure R1243zf

Thermal conductivity measurements of pure R1243zf were carried out in the temperature range from (314.2 to 405.6) K and pressures from (0.9 to 6.1) MPa in the homogeneous liquid and vapour phases. The experimental data (T, p, λ) of pure R1243zf are listed in Table 4. Overall, a total of 35 values of thermal conductivity were acquired in the range from (0.020 to

0.068) $W \cdot m^{-1} \cdot K^{-1}$ at densities from (32 to 964) $kg \cdot m^{-3}$. The pressure-temperature phase diagram of pure R1243zf showing the measurement conditions, the measured thermal conductivities, λ_{exp}, as a function of density, and the relative deviations of λ_{exp} from values calculated using the ECS model (Chichester and Huber, 2008) in REFPROP 10 (Lemmon et al., 2018) are illustrated in Figure 3. The relative deviations with the ECS model range from (–4 to 14) % in the gas phase and from (–5 to 11) % in the liquid phase.

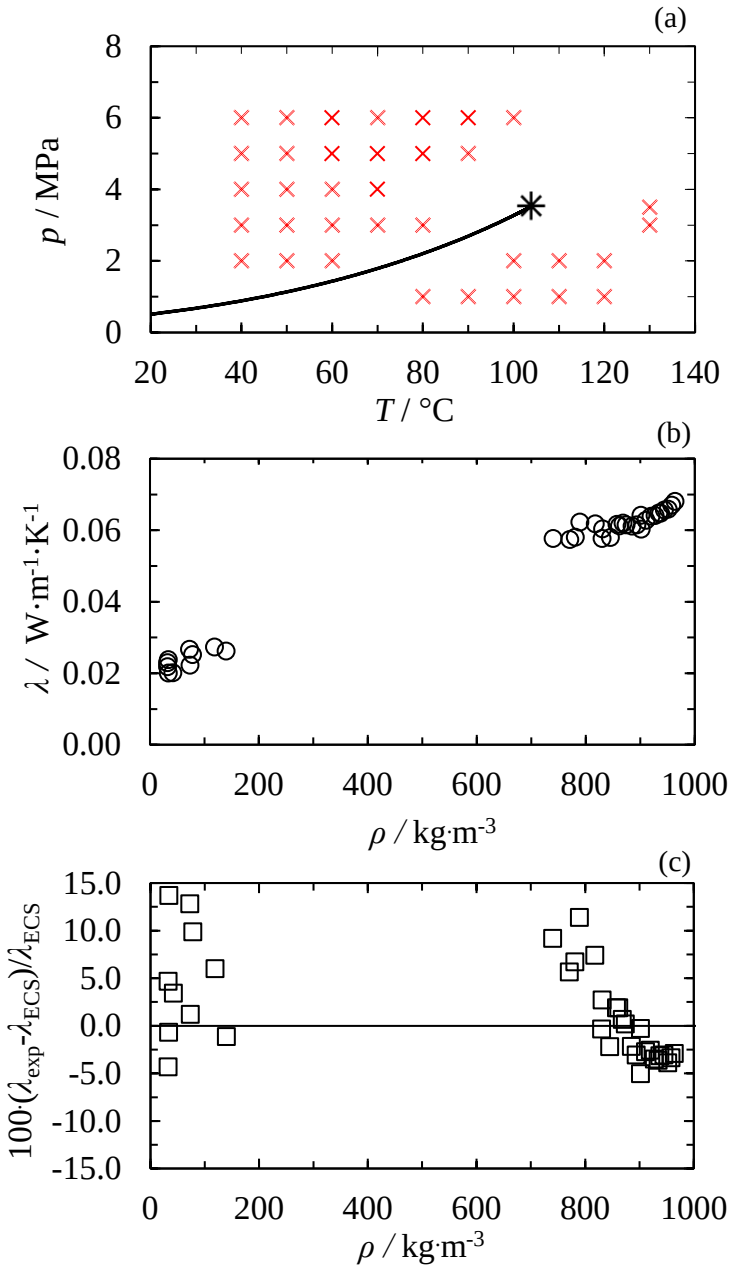

Figure 3. (a) The pressure-temperature phase diagram of R1243zf. ×, values measured in the this work; ✱, critical point; –, phase boundaries calculated with REFPROP 10 (Lemmon et al., 2018). (b) ○, the experimental thermal conductivity λ_{exp} as a function of density ρ (Akasaka, 2016); (c) □, relative deviations of λ_{exp} from values λ_{ECS} calculated with the ECS model (Chichester and Huber, 2008).

Table 4. Thermal conductivity data λ_{exp} measured for the pure R1243zf with the combined expanded uncertainty (k = 2) $U_c(\lambda)$[a] and fluid density ρ_{EoS} calculated from the measured temperature and pressure.[b]

T /K	p /MPa	ρ_{EoS} /(kg·m^{-3})	λ_{exp} /(W·m^{-1}K^{-1})	$U_C(\lambda)$ /(W·m^{-1}K^{-1})	T /K	p /MPa	ρ_{EoS} /(kg·m^{-3})	λ_{exp} /(W·m^{-1}K^{-1})	$U_C(\lambda)$ /(W·m^{-1}K^{-1})
Liquid phase									
314.16	2.078	937.21	0.0648	0.0014	334.31	5.041	893.48	0.0616	0.0049
314.20	3.080	944.37	0.0657	0.0018	334.64	6.047	901.16	0.0642	0.0065
314.21	4.116	951.32	0.0660	0.0010	344.49	3.042	829.95	0.0578	0.0020
314.20	5.094	957.52	0.0671	0.0008	344.46	4.074	844.85	0.0581	0.0021
314.20	6.118	963.59	0.0682	0.0017	344.43	5.057	857.02	0.0617	0.0024
324.16	1.999	901.36	0.0604	0.0014	344.41	6.065	867.96	0.0621	0.0051
324.20	2.995	910.41	0.0628	0.0020	354.23	3.084	780.60	0.0581	0.0024
324.27	4.108	919.44	0.0640	0.0020	354.35	5.096	817.31	0.0619	0.0041
324.31	5.093	926.82	0.0642	0.0011	354.46	6.096	830.74	0.0605	0.0028
324.24	6.056	933.88	0.0649	0.0019	364.40	5.103	770.38	0.0575	0.0023
334.15	2.019	861.58	0.0613	0.0021	364.50	6.107	788.91	0.0623	0.0050
334.17	3.026	873.71	0.0616	0.0020	374.67	6.110	739.72	0.0578	0.0042
334.19	4.086	884.85	0.0612	0.0012					
Gas phase									
355.67	1.101	42.01	0.02021	0.00170	386.13	2.038	77.82	0.02528	0.00260
365.70	0.937	33.31	0.02013	0.00257	395.66	0.999	32.03	0.02193	0.00252
373.83	0.971	33.62	0.02387	0.00144	396.35	2.010	72.36	0.02679	0.00412
376.15	1.846	73.25	0.02235	0.00207	405.62	3.011	118.39	0.02744	0.00305
385.58	0.976	32.33	0.02305	0.00396	404.57	3.339	139.68	0.02632	0.00188

[a] The expanded uncertainties (k = 2) of the measurements are 0.10 K for temperature T and 0.04 MPa for pressure p. [b] ρ_{EoS} is the density calculated with the reference EoS (Akasaka, 2016) implemented in the REFPROP 10 (Lemmon et al., 2018).

4.3. Measurement results for R32 binary mixtures

The experimental (T, p, λ) data of the (R32 + R1234yf) and (R32 + R1243zf) mixtures are presented in Table 5 and Table 6. Overall, a total of 73 values of thermal conductivity for six mixtures were acquired in the range from (0.015 to 0.123) W·m^{-1}·K^{-1} at densities from (23 to 1184) kg·m^{-3}. A few experiments in the liquid phase were conducted twice to check the repeatability of the measurements. Densities for the two binary systems were calculated using each mixture's Helmholtz equation of state (EoS) implemented in the REFPROP 10 (Lemmon et al., 2018).

Table 5. Thermal conductivity λ_{exp} data measured for the (R32 + R1234yf) mixtures with the combined expanded uncertainty (k = 2) $U_C(\lambda)$[a] and mixture density, ρ_{EoS}, calculated from the measured temperature and pressure.[b]

T /K	p /MPa	ρ_{EoS} /(kg·m^{-3})	λ_{exp} /(W·m^{-1}K^{-1})	$U_C(\lambda)$ /(W·m^{-1}K^{-1})	T /K	p /MPa	ρ_{EoS} /(kg·m^{-3})	λ_{exp} /(W·m^{-1}K^{-1})	$U_C(\lambda)$ /(W·m^{-1}K^{-1})
Vapour Phase					Liquid Phase				
0.750 R32 + 0.250 R1234yf									
314.86	0.903	26.20	0.01495	0.00024	264.25	1.945	1128.13	0.1151	0.0024
335.14	0.885	23.43	0.01666	0.00029	284.28	1.947	1056.17	0.1011	0.0024
334.51	1.876	56.59	0.01703	0.00024	284.26	2.929	1061.55	0.1009	0.0021
354.83	1.758	46.86	0.01896	0.00047	304.37	2.969	977.75	0.0906	0.0022
354.01	2.846	86.65	0.01978	0.00058	304.36	3.986	986.23	0.0933	0.0025
374.54	2.747	73.02	0.01925	0.00032	314.01	3.933	939.66	0.0828	0.0017
					324.24	3.935	881.16	0.0737	0.0016
0.500 R32 + 0.500 R1234yf									
325.74	1.067	37.86	0.01560	0.00026	274.20	1.959	1124.92	0.0889	0.0017
345.67	0.995	31.92	0.01786	0.00029	299.28	1.995	1027.00	0.0756	0.0016
345.23	1.950	71.45	0.01784	0.00025	299.30	2.999	1035.06	0.0775	0.0014
365.59	2.012	66.22	0.02066	0.00037	314.22	2.972	965.37	0.0708	0.0014
					314.57	3.997	975.33	0.0690	0.0017
					324.30	3.969	923.88	0.0701	0.0012
0.252 R32 + 0.748 R1234yf									
334.65	1.020	41.89	0.01707	0.00028	264.41	1.540	1183.74	0.0801	0.0014
354.75	1.010	37.82	0.01835	0.00028	284.22	1.490	1116.38	0.0716	0.0012
354.43	1.877	80.14	0.01763	0.00027	284.17	2.428	1122.03	0.0735	0.0015
373.92	1.997	77.57	0.01993	0.00030	304.20	2.509	1046.05	0.0626	0.0013
385.21	2.320	88.28	0.02277	0.00039	304.15	3.503	1054.53	0.0643	0.0011
394.77	2.492	91.90	0.02140	0.00034	314.09	3.465	1012.42	0.0606	0.0010
					324.25	3.500	964.58	0.0558	0.0009

[a] The expanded uncertainties (k = 2) of the measurements are 0.10 K for temperature T and 0.04 MPa for pressure p, while those for the mixture compositions are summarized in Table 2.
[b] ρ_{EoS} is the density calculated with the default Helmholtz equations of state for these mixtures implemented in the software package REFPROP 10 (Lemmon et al., 2018).

The experimental thermal conductivities of (R32 + R1234yf) were measured in the range from (0.015 to 0.023) W·m^{-1}·K^{-1} at densities from (23 to 92) kg·m^{-3} for the vapour phase and in the range from (0.056 to 0.115) W·m^{-1}·K^{-1} at densities from (881 to 1184) kg·m^{-3} for the liquid phase. The measured thermal conductivities are depicted as a function of density in Figure 4(a), and the relative deviations of the measured thermal conductivities from those calculated using the default ECS model were between (−14 and 2) %, as shown in Figure 4(b). The experimental thermal conductivities measured for (R32 + R1234yf) were compared with data from the literature (Miyara et al., 2011). These comparisons are shown in terms of the relative deviations of the data from thermal conductivities calculated with the default ECS model**.** Our measurements are generally within the scatter of the literature data in the liquid phase. Additionally, the modified binary interaction parameters for the (R32 + R1234yf) system suggested by Arami-Niya et al. (2020) and Kim et al. (2020) for the Helmholtz EOS and ECS

models, respectively, were used to improve the thermal conductivity predictions, with the relative deviations shown as a function of density in Figure 4(c). Using the optimised binary interaction parameters rather than the default values reduced the root mean square deviations for the liquid phase thermal conductivity data from (7.9 to 3.9) %.

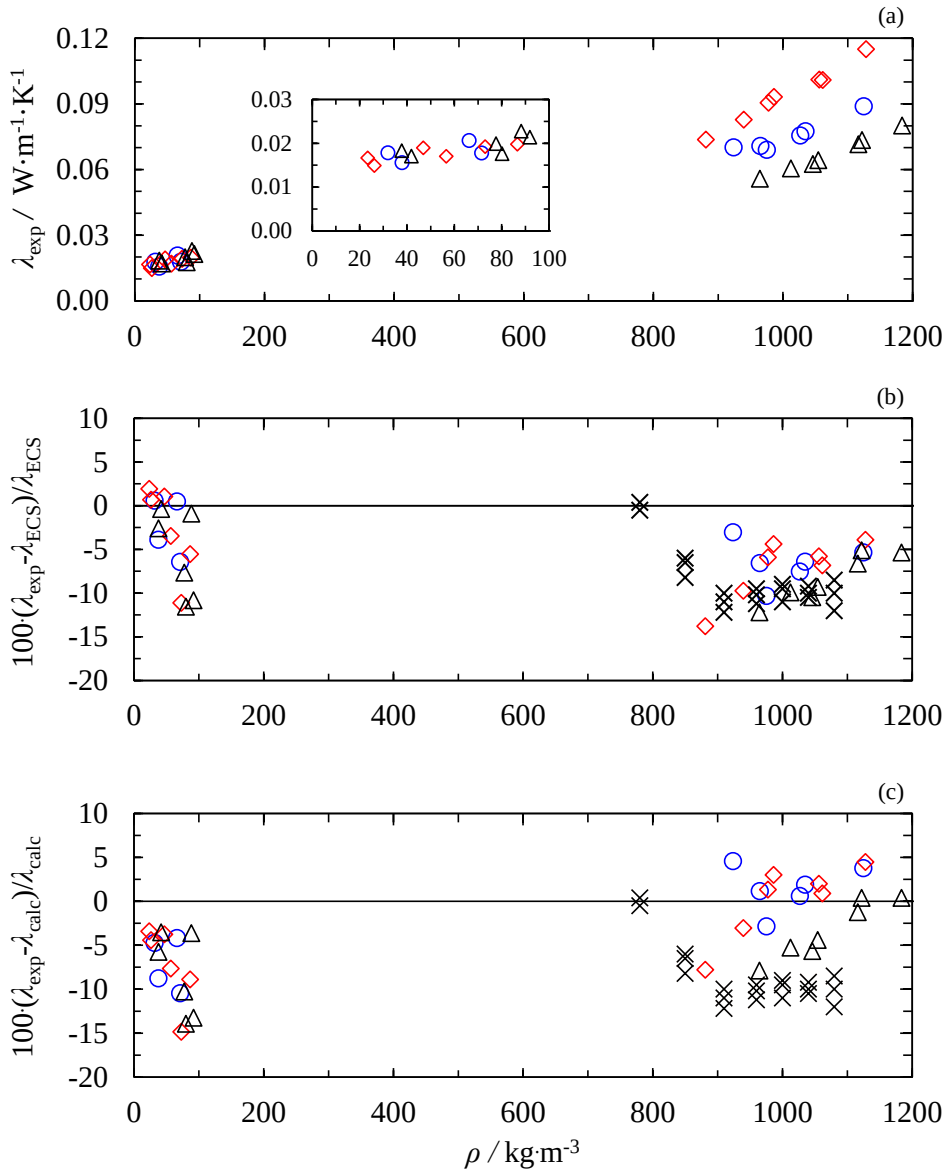

Figure 4. (a) The measured thermal conductivity λ_{exp} of the (R32 + R1234yf) mixtures as a function of density ρ. (b), (c) Relative deviations of λ_{exp} from values calculated with the default ECS model, λ_{ECS} (Chichester and Huber, 2008), and those calculated using the optimized BIPs, λ_{calc}, suggested by Arami-Niya et al. (2020) and Kim et al. (2020), respectively. Symbols: ◇, 0.750 R32 + 0.250 R1234yf, ○, 0.500 R32 + 0.500 R1234yf, △, 0.252 R32 + 0.748 R1234yf in this work; ×, Miyara et al. (2011) (Miyara et al., 2011).

Table 6. Thermal conductivity λ_{exp} data measured for the (R32 + R1243zf) mixtures with the combined expanded uncertainty (k = 2) $U_C(\lambda)$[a] and mixture density, ρ_{EoS}, calculated from the measured temperature and pressure.[b]

T /K	p /MPa	ρ_{EoS} /(kg·m^{-3})	λ_{exp} /(W·m^{-1}K^{-1})	$U_C(\lambda)$ /(W·m^{-1}K^{-1})	T /K	p /MPa	ρ_{EoS} /(kg·m^{-3})	λ_{exp} /(W·m^{-1}K^{-1})	$U_C(\lambda)$ /(W·m^{-1}K^{-1})
Vapour Phase					Liquid Phase				
0.750 R32 + 0.250 R1243zf									
324.66	1.020	26.85	0.01576	0.00030	264.16	1.882	1073.71	0.1228	0.0022
325.03	1.586	45.31	0.01621	0.00022	284.08	1.995	1007.66	0.1103	0.0024
345.19	1.046	25.27	0.01769	0.00026	283.97	3.000	1013.02	0.1133	0.0022
344.83	1.970	52.98	0.01899	0.00053	304.02	3.018	935.79	0.0990	0.0019
364.80	2.038	49.84	0.02090	0.00051	303.93	3.990	943.40	0.1011	0.0019
385.57	4.041	106.44	0.02748	0.00054	313.92	3.984	899.52	0.0957	0.0017
					324.04	3.971	846.93	0.0862	0.0021
0.500 R32 + 0.500 R1243zf									
334.46	1.043	31.59	0.01617	0.00027	264.12	1.510	1067.96	0.1005	0.0021
354.50	1.053	29.32	0.01769	0.00024	284.08	1.486	1005.19	0.0890	0.0015
354.05	1.958	61.10	0.01793	0.00032	284.08	2.541	1010.59	0.0908	0.0020
374.18	2.038	57.82	0.01883	0.00033	303.95	2.509	938.95	0.0800	0.0014
373.91	2.531	75.92	0.01971	0.00040	303.99	3.496	946.17	0.0805	0.0013
394.29	2.413	64.63	0.02034	0.00033	313.80	3.441	906.18	0.0759	0.0016
					323.84	3.541	860.75	0.0703	0.0011
0.248 R32 + 0.752 R1243zf									
344.46	1.164	40.50	0.01817	0.00030	298.88	1.443	964.54	0.0738	0.0013
364.47	1.052	32.98	0.02008	0.00031	298.89	2.461	971.12	0.0742	0.0018
364.51	1.998	71.47	0.01923	0.00027	313.92	2.506	917.60	0.0692	0.0010
384.79	2.038	65.65	0.02322	0.00038	314.00	3.521	925.91	0.0684	0.0014
395.38	3.086	106.37	0.02349	0.00034	323.94	3.443	886.39	0.0674	0.0012
					334.05	3.499	841.74	0.0630	0.0014

[a] The expanded uncertainties (k = 2) of the measurements are 0.10 K for temperature T and 0.04 MPa for pressure p, while those for the mixture compositions are summarized in Table 2.
[b] ρ_{EoS} is the density calculated with the default Helmholtz equations of state for these mixtures implemented in the software package REFPROP 10 (Lemmon et al., 2018).

Measurements of the thermal conductivity of (R32 + R1243zf) were conducted in the range from (0.016 to 0.027) W·m^{-1}·K^{-1} at densities from (25 to 106) kg·m^{-3} for the vapour phase and in the range from (0.063 and 0.123) W·m^{-1}·K^{-1} at densities from (842 to 1074) kg·m^{-3} for the liquid phase. The measured thermal conductivities are depicted as a function of density in Figure 5(a). The relative deviations of the measured thermal conductivities from those calculated using the ECS model were between (−13 and +10) % as shown in Figure 5(b). The relative deviations become increasingly around 100 kg·m^{-3} as the mixture critical point is approached.

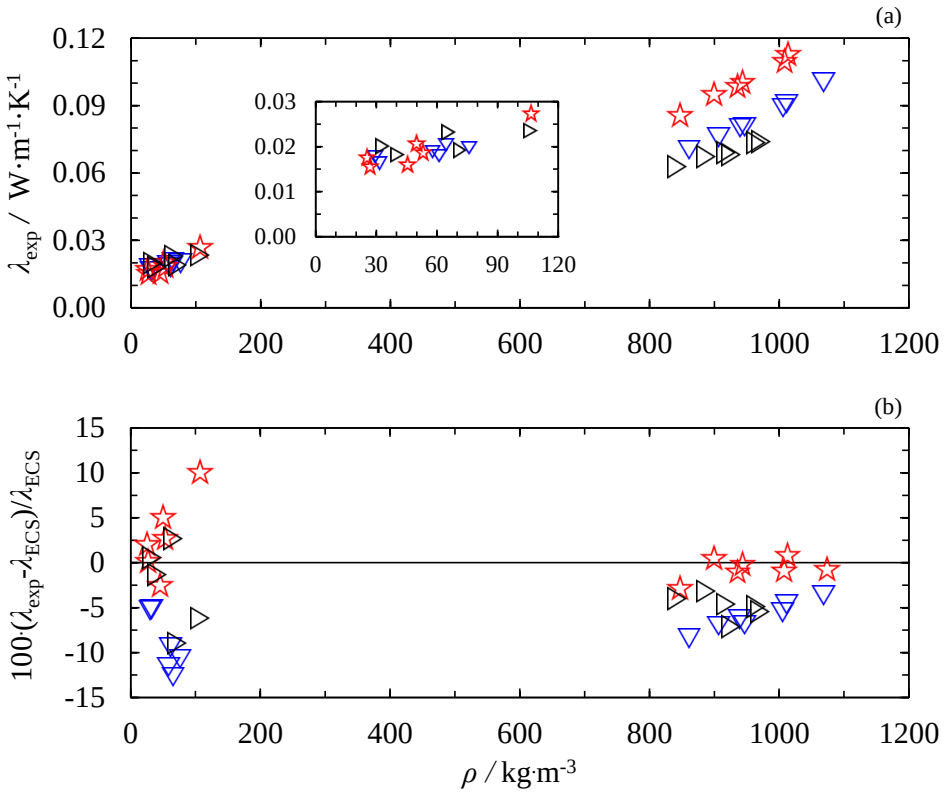

Figure 5. (a) The measured thermal conductivity λ_{exp} of the (R32 + R1234yf) mixtures as a function of density ρ. (b) Relative deviations of λ_{exp} of these mixtures from values calculated with the ECS model λ_{ECS} (Chichester and Huber, 2008), as function of densities. Symbols: ☆, 0.750 R32 + 0.250 R1243zf; ▽, 0.500 R32 + 0.500 R1243zf; ▷, 0.248 R32 + 0.752 R1243zf.

4.4 Comparison with RES-CPA model

The thermal conductivities of R1243zf measured in this work were the only data available for the fitting of the rescaling parameter ζ for this pure fluid. With $\zeta_{R1243zf}$ = 1.0356, the thermal conductivities for R1243zf are reasonably well-described by the 'universal' RES curve, as shown in Figure 6(a). For R32 and R1234yf, the parameters of the CPA EoS and binary interaction parameter (k_{ij} = 0.0549) were obtained from (Yang et al., 2019), and the parameters of the RES-CPA thermal conductivity model were obtained from Liu et al. (2021) (Liu et al., 2021). For R1243zf, the parameters of the CPA EoS were obtained from Yang et al (Yang et al., 2019). Experimental data for the equilibrium properties of relevant mixtures containing R1243zf are not available. Thus, the van der Waals binary interaction parameter, k_{ij}, was estimated to be the same value as the (R32 + R1234yf) binary mixture given the similarity of the R1234yf and R1243zf molecules. The thermal conductivity data for the binary mixtures, (R32 + R1234yf) and (R32 + R1243zf), are also represented well by the RES curve shown in Figure 6(a), with no fitting or parameter adjustment applied.

The relative deviations of the experimental data from the RES-CPA model for pure R1243zf, R32 + R1234yf, and R32 + R1243zf are shown in Figure 6(b), (c) and (d), respectively. The

RES-CPA model is able to predict with the experimental thermal conductivities measured for R32 + R1234yf within (–12 to +4) %, and, for R32 + R1243zf, within (–12 to +9) %. These deviations are similar in magnitude to those observed for the ECS model but with significantly fewer adjustable parameters.

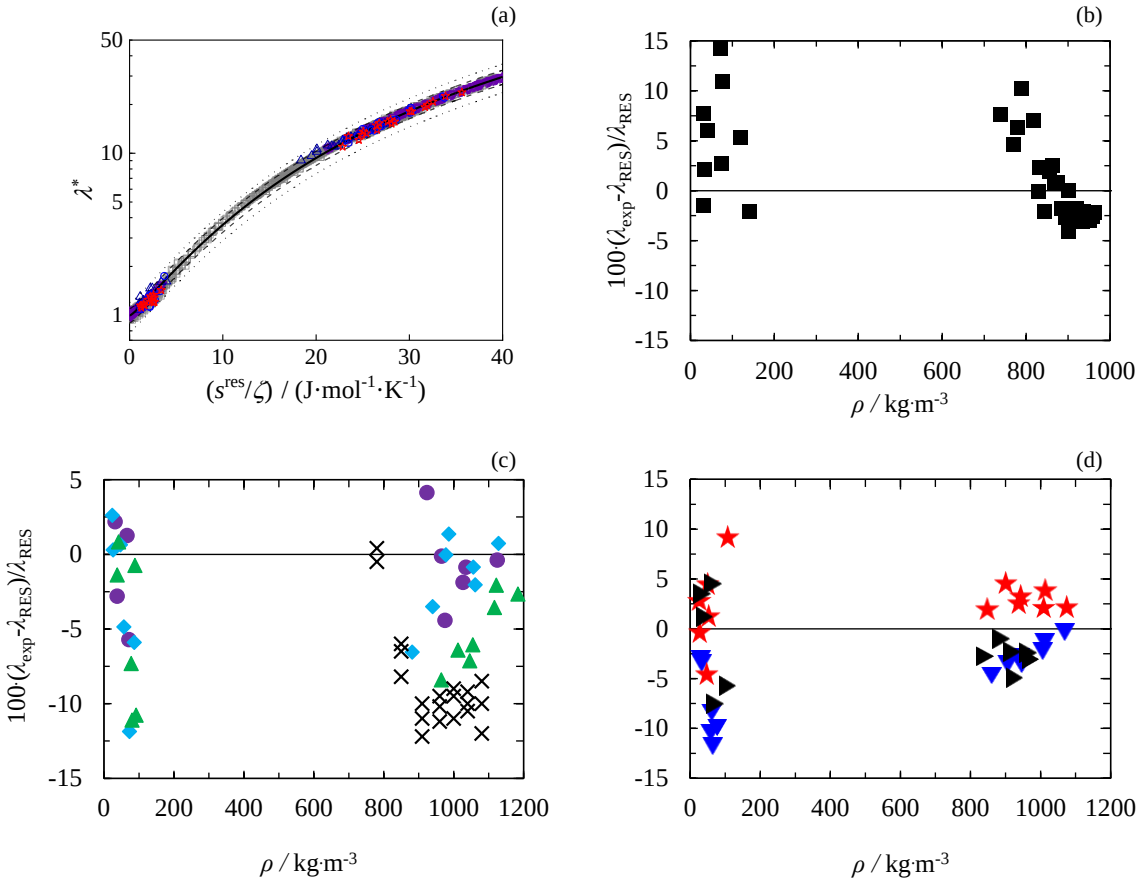

Figure 6. (a) Reduced thermal conductivity λ^* *vs* residual entropy s^{res}/ζ. Symbols: □ R32, ▽ R1234yf, △ R1243zf, ☆ R32 + R1234yf, ○ R32 + R1243zf, – RES correlation, --- 10% deviation from RES correlation, - - - 20% deviation from RES correlation. Relative deviations of the experimental thermal conductivities λ_{exp} for (b) pure R1243zf, (c) R32 + R1234yf mixtures and (d) R32 + R1243zf mixtures from values λ_{RES} calculated with the RES-CPA model as function of density ρ. Symbols: ■, R1243zf; ◆, 0.750 R32 + 0.250 R1234yf; ●, 0.500 R32 + 0.500 R1234yf; ▲, 0.252 R32 + 0.748 R1234yf; ★, 0.750 R32 + 0.250 R1243zf; ▼, 0.500 R32 + 0.500 R1243zf; ▶, 0.248 R32 + 0.752 R1243zf in this work; ×, Miyara et al. (Miyara et al., 2011).

5. Conclusions

In this paper, we report experimental thermal conductivity data for pure R1243zf and two binary systems, R32+R1234yf and R32+R1243zf with molar fractions 0.25, 0.50 and 0.75 of R32. The thermal conductivity in the homogenous vapour and liquid phases was measured using the transient hot wire technique in the temperature range from (264.1 to 405.6) K with pressures ranging between (0.9 and 6.1) MPa. The relative combined expanded uncertainty (k = 2) in the experimental thermal conductivity was approximately 2.0%. The relative deviations of the measured thermal conductivities from the default extended corresponding states (ECS) model, which is implemented in the REFPROP 10, were between (−13 and +10)% in the vapour phase and between (−14 and +1)% in the liquid phase. For R32+R1234yf mixtures, using the improved interaction parameters suggested by Arami-Niya et al. (2020) and Kim et al. (2020) **,** for the Helmholtz and ECS models implemented in REFPROP 10 reduced the RMS difference between measured and predicted liquid phase thermal conductivities from (7.9 to 3.9) %.

Additionally, the parameters of the residual entropy scaling model incorporating cubic-plus-association equation of state (RES-CPA model) for the thermal conductivity of pure R1243zf and binary R32+R1243zf system were determined. The measured pure and mixture data can then be readily mapped onto a univariate function of the residual entropy through the RES approach. The RES-CPA model predicts the experimental mixture thermal conductivities generally within 10%, which is similar to the ECS model but is achieved with no binary-specific adjustable parameters.

Acknowledgments

This work was supported by the Australian Research Council through IC150100019 and the National Natural Science Foundation of China [Grant No. 51736005].

References

Abas, N., Kalair, A.R., Khan, N., Haider, A., Saleem, Z., Saleem, M.S., 2018. Natural and synthetic refrigerants, global warming: A review. Renewable and Sustainable Energy Reviews 90, 557-569.

Akasaka, R., 2016. Recent trends in the development of Helmholtz energy equations of state and their application to 3, 3, 3-trifluoroprop-1-ene (R-1243zf). Science and Technology for the Built Environment 22, 1136-1144.

Al Ghafri, S.Z.S., Rowland, D., Akhfash, M., Arami-Niya, A., Khamphasith, M., Xiao, X., Tsuji, T., Tanaka, Y., Seiki, Y., May, E.F., 2019. Thermodynamic properties of hydrofluoroolefin (R1234yf and R1234ze (E)) refrigerant mixtures: Density, vapour-liquid equilibrium, and heat capacity data and modelling. Int. J. Refrig. 98, 249-260.

Arami-Niya, A., Xiao, X., Al Ghafri, S., Jiao, F., Khamphasith, M., Pouya, E.S., Seyyedsadaghiani, M., Yang, X., Tsuji, T., Tanaka, Y., 2020. Measurement and modelling of the thermodynamic properties of carbon dioxide mixtures with HFO-1234yf, HFC-125, HFC-134a, and HFC-32: vapour-liquid equilibrium, density, and heat capacity. Int. J. Refrig. 118, 514-528.

Assael, M.J., Antoniadis, K.D., Wakeham, W.A., 2010. Historical evolution of the transient hot-wire technique. International journal of thermophysics 31, 1051-1072.

Assael, M.J., Nieto de Castro, C.A., Roder, H.M., Wakeham, W.A., 1991. Transient methods for thermal conductivity. Experimental Thermodynamics 3, 161-195.

Bell, I.H., 2020. Entropy Scaling of Viscosity—I: A Case Study of Propane. J. Chem. Eng. Data 65, 3203–3215.

Calm, J.M., 2008. The next generation of refrigerants–Historical review, considerations, and outlook. Int. J. Refrig. 31, 1123-1133.

Chichester, J.C., Huber, M.L., 2008. Documentation and Assessment of the Transport Property Model for Mixtures Implemented in NIST REFPROP (Version 8.0). National Institute of Standards and Technology.

Fouad, W.A., 2020. Thermal Conductivity of Pure Fluids and Multicomponent Mixtures Using Residual Entropy Scaling with PC-SAFT—Application to Refrigerant Blends. J. Chem. Eng. Data 65, 5688-5697.

Gil, B., Kasperski, J., 2018. Efficiency evaluation of the ejector cooling cycle using a new generation of HFO/HCFO refrigerant as a R134a replacement. Energies 11, 2136.

Higashi, Y., Sakoda, N., Islam, M.A., Takata, Y., Koyama, S., Akasaka, R., 2018. Measurements of saturation pressures for trifluoroethene (R1123) and 3, 3, 3-trifluoropropene (R1243zf). Journal of Chemical & Engineering Data 63, 417-421.

Hopp, M., Gross, J., 2019. Thermal conductivity from entropy scaling: a group-contribution method. Ind. Eng. Chem. Res. 58, 20441-20449.

ISO, I., OIML, B., 1995. Guide to the Expression of Uncertainty in Measurement. Geneva, Switzerland.

Kim, D., Yang, X., Arami-Niya, A., Rowland, D., Xiao, X., Al Ghafri, S., Tsuji, T., Tanaka, Y., Seiki, Y., May, E.F., 2020. Thermal conductivity measurements of refrigerant mixtures containing hydrofluorocarbons (HFC-32, HFC-125, HFC-134a), hydrofluoroolefins (HFO-1234yf), and carbon dioxide (CO2). The Journal of Chemical Thermodynamics, 106248.

Kujak, S., Schultz, K., 2016. Insights into the next generation HVAC&R refrigerant future. Science and Technology for the Built Environment 22, 1226-1237.

Lai, N.A., 2014. Thermodynamic properties of HFO-1243zf and their application in study on a refrigeration cycle. Applied thermal engineering 70, 1-6.

Lemmon, E.W., Bell, I.H., Huber, M.L., McLinden, M.O., 2018. NIST Standard Reference Database 23: Reference Fluid Thermodynamic and Transport Properties-REFPROP, Version 10.0, National Institute of Standards and Technology. 2018. URL http://www. nist. gov/srd/nist23. cfm.

Liu, H., Yang, F., Yang, X., Yang, Z., Duan, Y., 2021. Modeling the thermal conductivity of hydrofluorocarbons, hydrofluoroolefins and their binary mixtures using residual entropy scaling and cubic-plus-association equation of state. Journal of Molecular Liquids 330, 115612.
Liu, H., Yang, F., Yang, Z., Duan, Y., 2020. Modeling the viscosity of hydrofluorocarbons, hydrofluoroolefins and their binary mixtures using residual entropy scaling and cubic-plus-association equation of state. Journal of Molecular Liquids 308, 113027.
McLinden, M.O., Klein, S.A., Perkins, R.A., 2000. An extended corresponding states model for the thermal conductivity of refrigerants and refrigerant mixtures. International Journal of Refrigeration 23, 43-63.
Miyara, R., Fukuda, K., Tsubaki, 2011. Trans. Japan Soc. Refrig. Air Condit. Eng. 28, 435–443.
Mylona, S.K., Hughes, T.J., Saeed, A.A., Rowland, D., Park, J., Tsuji, T., Tanaka, Y., Seiki, Y., May, E.F., 2019. Thermal conductivity data for refrigerant mixtures containing R1234yf and R1234ze (E). The Journal of Chemical Thermodynamics 133, 135-142.
Mylona, S.K., Yang, X., Hughes, T.J., White, A.C., McElroy, L., Kim, D., Al Ghafri, S., Stanwix, P.L., Sohn, Y.H., Seo, Y., May, E.F., 2020. High-Pressure Thermal Conductivity Measurements of a (Methane + Propane) Mixture with a Transient Hot-Wire Apparatus. Journal of Chemical & Engineering Data 65, 906-915.
Neufeld, P.D., Janzen, A.R., Aziz, R.A., 1972. Empirical equations to calculate 16 of the transport collision integrals Ω (l, s)* for the Lennard - Jones (12 – 6) potential. The Journal of Chemical Physics 57, 1100-1102.
Pachauri, R.K., Allen, M.R., Barros, V.R., Broome, J., Cramer, W., Christ, R., Church, J.A., Clarke, L., Dahe, Q., Dasgupta, P., Dubash, N.K., 2014. Climate change 2014: synthesis report. Contribution of Working Groups I, II and III to the fifth assessment report of the Intergovernmental Panel on Climate Change. IPCC, 151.
Pal, A., Uddin, K., Thu, K., Saha, B.B., 2018. Environmental assessment and characteristics of next generation refrigerants. Kyushu University.
Perkins, R.A., Huber, M.L., Assael, M.J., 2016. Measurements of the thermal conductivity of 1, 1, 1, 3, 3-Pentafluoropropane (R245fa) and correlations for the viscosity and thermal conductivity surfaces. J. Chem. Eng. Data 61, 3286-3294.
Perkins, R.A., Roder, H.M., Nieto de Castro, C.A., 1991. A high-temperature transient hot-wire thermal conductivity apparatus for fluids. Journal of research of the National Institute of Standards and Technology 96, 247-269.
Sadaghiani, M.S., Arami-Niya, A., Zhang, D., Tsuji, T., Tanaka, Y., Seiki, Y., May, E.F., 2021. Minimum ignition energies and laminar burning velocities of ammonia, HFO-1234yf, HFC-32 and their mixtures with carbon dioxide, HFC-125 and HFC-134a. Journal of Hazardous Materials 407, 124781.
Webb, R.L., 1981. Performance evaluation criteria for use of enhanced heat transfer surfaces in heat exchanger design. International Journal of Heat and Mass Transfer 24, 715-726.
Wu, X., Dang, C., Xu, S., Hihara, E., 2019. State of the art on the flammability of hydrofluoroolefin (HFO) refrigerants. International Journal of Refrigeration 108, 209-223.
Yang, F., Chu, Q., Liu, Q., Duan, Y., Yang, Z., 2019. The cubic-plus-association equation of state for hydrofluorocarbons, hydrofluoroolefins, and their binary mixtures. Chemical Engineering Science 209, 115182.
Yang, X., Arami-Niya, A., Xiao, X., Kim, D., Ghafri, S.A., Tsuji, T., Tanaka, Y., Seiki, Y., May, E.F., 2020a. Viscosity measurements of binary and multi-component refrigerant mixtures containing HFC-32, HFC-125, HFC-134a, HFO-1234yf and CO2. Journal of chemical & engineering data.
Yang, X., Liu, H., Chen, S.H., Kim, D., Yang, F., Arami-Niya, A., Duan, Y., 2021. Viscosity of binary refrigerant mixtures of R32 + R1234yf and R32 + R1243zf. Int. J. Refrig., (doi.org/10.1016/j.ijrefrig.2020.1011.1020).
Yang, X., Xiao, X., May, E.F., Bell, I.H., 2020b. Entropy Scaling of Viscosity -- III: Application to Refrigerants and their Mixtures. J. Chem. Eng. Data 66, 1385–1398.

Zilio, C., Brown, J.S., Schiochet, G., Cavallini, A., 2011. The refrigerant R1234yf in air conditioning systems. Energy 36, 6110-6120.

Graphical abstract

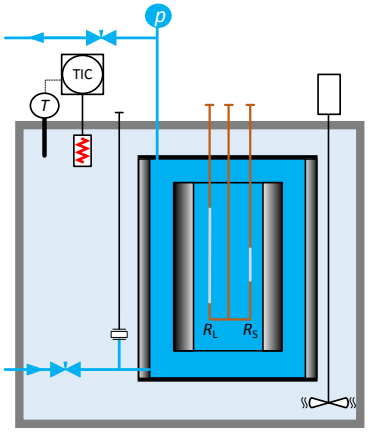

Measurements for HFC-32 mixtures with Transient Hot-Wire

Refrigerant mixtures with 0.75/0.50/0.25 ratio (HFC–32+HFO–1234yf/HFO–1243zf)

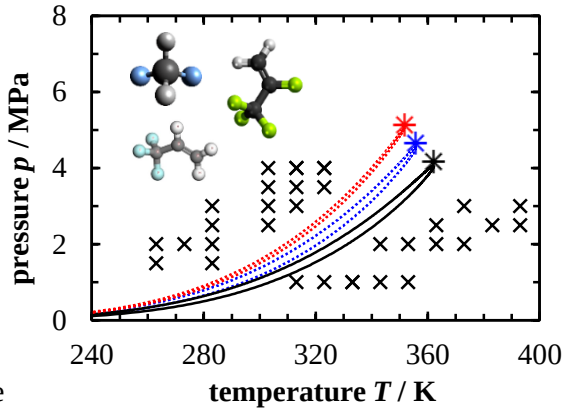

Credit Author Statement